E2 ubiquitin-conjugating enzymes, UBE2D1 and UBE2D2, regulate VEGFR2 dynamics and endothelial function

William R. Critchley[1], Gina A. Smith[1], Ian C. Zachary[2], Michael A. Harrison[3], Sreenivasan Ponnambalam[1,*]

[1]Endothelial Cell Biology Unit, School of Molecular and Cellular Biology, University of Leeds, Leeds, UK
[2]Centre for Cardiovascular Biology & Medicine, Rayne Building, University College London, London, UK
[3]School of Biomedical Sciences, University of Leeds, Leeds, UK

*Corresponding author email: s.ponnambalam@bmb.leeds.ac.uk

Summary Statement: New blood vessel sprouting is dependent on VEGFR2-regulated signal transduction. We show that ubiquitin-conjugating enzymes, UBE2D1 and UBE2D2, modulate VEGFR2 levels.

Abstract

Vascular endothelial growth factor receptor 2 (VEGFR2) regulates endothelial function and angiogenesis. VEGFR2 undergoes ubiquitination which programs this receptor for trafficking and proteolysis but the ubiquitin-modifying enzymes involved are ill-defined. Herein, we used a reverse genetics screen of the human E2 family of ubiquitin-conjugating enzymes to identify gene products which regulate VEGFR2 ubiquitination and proteolysis. We find that depletion of either UBE2D1 or UBE2D2 in endothelial cells cause a rise in steady-state VEGFR2 levels. This rise in plasma membrane VEGFR2 levels impact on VEGF-A-stimulated signalling, with increased activation of canonical MAPK, phospholipase Cγ1, and Akt pathways. Analysis of biosynthetic VEGFR2 is consistent with a role for UBE2D enzymes in influencing plasma membrane VEGFR2 levels. Cell surface biotinylation and recycling studies show an increase in VEGFR2 recycling to the plasma membrane upon reduction in UBE2D levels. Depletion of either UBE2D1 or UBE2D2 stimulates endothelial tubulogenesis which is consistent with increased VEGFR2 plasma membrane levels promoting the cellular response to exogenous VEGF-A. Our studies identify a key role for UBE2D1 and UBE2D2 in regulating VEGFR2 function in angiogenesis.

Keywords: VEGFR2, endothelial, ubiquitin, UBE2D1, UBE2D2, signalling, angiogenesis

Abbreviations: vascular endothelial growth factor A, VEGF-A; vascular endothelial growth factor receptor 2, VEGFR2; E1 ubiquitin-like modifier activating enzyme, UBA1; E2 ubiquitin-conjugating enzyme 2D1, UBE2D1; E2 ubiquitin-conjugating enzyme 2D2, UBE2D2;

Introduction

Angiogenesis describes new blood vessel sprouting from pre-existing ones; this is essential for vascular homeostasis, wound healing and revascularisation. Dysregulated angiogenesis is a major factor in disease pathologies including diabetic retinopathy (Martin et al., 2003), cardiovascular disease (Khurana et al., 2005) and tumour growth (De Palma et al., 2017). Soluble pro-angiogenic factors bind to membrane-bound receptors on the endothelium and activate multiple signalling pathways resulting in angiogenesis. However, we lack mechanism(s) explaining how receptor-ligand dynamics regulate endothelial responses in spite of identification of many angiogenic regulators. A major pro-angiogenic cytokine, vascular endothelial growth factor A (VEGF-A), secreted by many cell types exerts its pro-angiogenic effects by predominantly interacting with VEGFR2, a receptor tyrosine kinase (Chung and Ferrara, 2011). VEGF-A stimulates VEGFR2 tyrosine autophosphorylation, receptor internalization and activation of multiple signal transduction pathways: these events promote endothelial cell migration, proliferation and tubulogenesis (Ewan et al., 2006; Fearnley et al., 2016).

It is well-established that VEGFR2 undergoes proteolysis linked to ubiquitination (Bruns et al., 2010; Duval et al., 2003) but the underlying regulatory mechanism is unclear. Previous studies show a role for the major E1 ubiquitin activating enzyme, UBA1 in regulating VEGFR2 ubiquitination (Smith et al., 2017). Although a variety of E3 ubiquitin ligases including c-Cbl, βTrcP, RNF121 and Nedd4 (Duval et al., 2003; Maghsoudlou et al., 2016; Murdaca et al., 2004; Sakaue et al., 2017; Shaik et al., 2012) are postulated to target VEGFR2, we have lacked a logical framework which provides a mechanism for VEGFR2 ubiquitination.

Ubiquitination in eukaryote species usually involves a tripartite system of ubiquitin-modifying enzymes such as E1 (ubiquitin-activating), E2 (ubiquitin-conjugating) and E3 (substrate recognition) that work in concert to conjugate ubiquitin onto one or more lysine residues within the protein substrate (Critchley et al., 2018; Scheffner et al., 1995).

Membrane proteins clearly undergo ubiquitination thus programming trafficking and proteolysis but we have lacked information on E2 ubiquitin-conjugating enzymes that regulate VEGFR2 dynamics. The complexity of the E2 ubiquitin-conjugating enzymes is highlighted by the 38 E2 members that facilitate ubiquitin conjugation to a wide variety of protein substrates.

To address this issue in the context of VEGFR2 ubiquitination and turnover, we developed a microscopy–based reverse genetics screen to evaluate E2 ubiquitin-conjugating enzyme requirement for VEGFR2 turnover in endothelial cells. Our previous studies established that the E1 enzyme, UBA1 and not UBA6, controls VEGFR2 ubiquitination which impacts on membrane protein trafficking and turnover which further regulates VEGF-A-stimulated endothelial responses (Smith et al., 2017). Herein, we used a reverse genetics approach to identify E2 ubiquitin-conjugating enzymes that control VEGFR2 levels, downstream signalling and endothelial responses. By screening the human E2 family, we discovered two closely related E2 ubiquitin-conjugating enzymes (UBE2D1, UBE2D2) required for VEGFR2 ubiquitination. Our findings demonstrate that UBE2D1 and UBE2D2 is required for VEGFR2 ubiquitination and proteolysis, thus modulating downstream VEGF-A-regulated signalling. Such effects impacts on VEGF-A-regulated tubulogenesis, a key requirement for angiogenesis.

Results

A reverse genetics screen of the E2 family identifies UBE2D1 and UBE2D2 as direct regulators of VEGFR2 levels

To screen the human E2 ubiquitin-conjugating family for roles in VEGFR2 ubiquitination, we first compiled a comprehensive database of ubiquitin-specific E2 enzymes to include all validated, putative and catalytically inactive forms. To identify the E2 enzymes required for VEGFR2 turnover, we used employed reverse genetics approach using siRNA-based knockdown of each candidate E2 protein. We have previously described a morphological assay to analyse effects on VEGFR2 levels and used a reverse genetics siRNA-based screen to screen the human E2 family (see Materials and Methods) (Smith et al., 2017).

Analysis of VEGFR2 levels in primary human endothelial cells depleted for each of the 38 E2 ubiquitin conjugating enzymes is depicted in histogram format (Figure 1A). The most significant effect was a 2-fold rise in VEGFR2 levels caused by UBE2D1 depletion (Figure 1A, 1B). Knockdown of a closely related homologue, UBE2D2 causes ~1.6-fold

rise in VEGFR2 levels (Figure 1A, 1B). Interestingly two other closely related homologues of the UBE2D subfamily, UBE2D3 and UBE2D4, had much lesser effects on VEGFR2 levels (Figure 1A). Notably, knockdown of UBE2Z, which can only be ubiquitin-primed by UBA6 and not UBA1, had no effect on VEGFR2 levels, consistent with our previous findings and validating the importance of E1-E2 specificity (Smith et al., 2017).

Endothelial cells display variation in steady-state VEGFR2 levels (Figure 1B). However, knockdown of either UBE2D1 or UBE2D2 as part of the E2 screen causes increased VEGFR2 levels (Figure 1B). We then compared effects of knockdown of the UBE2D subfamily i.e. UBE2D1, UBE2D2, UBE2D3 and UBE2D4 on VEGFR2 levels using immunoblotting (Figure 2A). UBE2D1 or UBE2D2 knockdown caused a clear rise in VEGFR2 levels, whereas UBE2D3 or UBE2D4 knockdown had no significant effects (Figure 2A). Quantification of these data showed that knockdown of either UBE2D1 or UBE2D2 produced ~3-fold increase in steady-state VEGFR2 levels; however, UBE2D3 or UBE2D4 knockdown had little or no effects compared to control (Figure 2B). Such findings support roles for both UBE2D1 and UBE2D2 in regulating VEGFR2 levels in endothelial cells.

As E2 ubiquitin conjugating enzymes interact with a number of client proteins, we next considered whether VEGFR2 levels were affected directly or indirectly. To address this point, we used antibodies to isolate UBE2D1 and UBE2D2 complexes from endothelial cell lysates. We detected co-precipitation of VEGFR2 but not transferrin receptor, another plasma membrane receptor, with UBE2D1 and UBE2D2 (Figure 2C). This occurred in the absence of exogenous VEGF-A (Figure 2C). VEGFR2-UBE2D2 complex formation is particularly evident (Figure 2C). Higher molecular weight ubiquitinated VEGFR2 species were also evident in both basal and VEGF-A stimulated conditions followed by UBE2D complex isolation (Figure 2C).

UBE2D1 and UBE2D2 regulation of VEGFR2 signal transduction and membrane trafficking

We then asked whether UBE2D1 or UBE2D2-mediated regulation of VEGFR2 levels impact on VEGF-A-regulated signal transduction pathways (Figure 3). VEGF-A binding stimulates VEGFR2 tyrosine kinase activity; one characteristic feature is the rapid appearance of the phosphotyrosine VEGFR2-pY1175 epitope within 5 min of VEGF-A addition, followed by a slower decline in VEGFR2-pY1175 levels (Figure 3A). Analysis of endothelial cells subjected to UBE2D1 or UBE2D2 knockdown showed an increase in VEGFR2-pY1175 levels (Figure 3A); this corresponds to >2-fold increase in VEGFR2-

pY1175 levels upon either UBE2D1 or UBE2D2 knockdown compared to control (Figure 3B). Comparison of different signal transduction pathways shows ~2-3-fold increase in VEGF-A-stimulated activation of Akt, PLCγ1 and ERK pathways upon either UBE2D1 or UBE2D2 knockdown (Figure 3B). There is little or no effect on VEGF-A-regulated p38 MAPK activation upon knockdown of either UBE2D1 or UBE2D2 (Figure 3B). These data support roles for UBE2D1 and UBE2D2 in controlling plasma membrane VEGFR2 dynamics that impact on VEGF-A-stimulated downstream signalling.

VEGFR2 undergoes endocytosis, delivery to endosomes followed by degradation or recycling back to the plasma membrane (Figure 4A) (Ewan et al., 2006; Gampel et al., 2006; Jopling et al., 2014; Lampugnani et al., 2006). To test whether either UBE2D1 or UBE2D2 knockdown modulates VEGFR2 degradation or recycling, we used an endosome-to-plasma membrane recycling assay that only detects VEGFR2 molecules that have undergone at least one round of endocytosis and recycling back to the plasma membrane (Figure 4B) (Jopling et al., 2011). Depletion of either UBE2D1 or UBE2D2 caused ~1.5-2-fold increase in the proportion of VEGFR2 recycled back to the plasma membrane compared to control untreated cells or in cells treated with VEGF-A (Figure 4C). Combining cell surface VEGFR2 biotinylation with inhibition of new protein synthesis (using cycloheximide) caused ~1.5-fold increase in mature VEGFR2 levels at the plasma membrane upon depletion of either UBE2D1 or UBE2D2 (Figure 4D, 4E).

Knockdown of either UBE2D1 or UBE2D2 elevates steady-state or basal VEGFR2 levels; one question is the intracellular location of VEGFR2 ubiquitination. To answer this, we combined cycloheximide treatment (to block biosynthetic VEGFR2 production) with UBE2D1 or UBE2D2 knockdown and assessed VEGFR2 levels. In control cells transfected with non-targeting siRNA, we observe a significant decrease in mature VEGFR2 levels (Figure 5A). In non-stimulated endothelial cells, mature VEGFR2 does not display tyrosine phosphorylation, but undergoes degradation over time (Figure 5A) corresponding to ~50% VEGFR2 decrease over 80 min (Figure 5B). Upon knockdown of either UBE2D1 or UBE2D2, mature VEGFR2 levels are initially higher but decline in a similar pattern to control (Figure 5A). For either UBE2D1 or UBE2D2 knockdown, the decrease in mature VEGFR2 levels displays similar kinetics to control (Figure 5B).

UBE2D1 or UBE2D2 depletion does not affect transferrin receptor levels; this membrane protein recycles between the plasma membrane and endosomes (Figure 5A). Immunofluorescence microscopy showed that knockdown of UBE2D1 or UBE2D2 followed by cycloheximide treatment to block new protein synthesis, causes widespread accumulation of VEGFR2 including at the plasma membrane and in endosomes (Figure

5C). Quantification of VEGFR2 staining shows ~3-fold rise in VEGFR2 levels caused by UBE2D1 or UBE2D2 knockdown; blocking new protein synthesis using cycloheximide causes only 10-20% reduction in VEGFR2 levels (Figure 5D). The knockdown of UBE2D1 and UBE2D2 thus causes mature VEGFR2 accumulation at the plasma membrane and endosomes.

UBE2D1 and UBE2D2 promote VEGFR2 down-regulation to regulate endothelial tubulogenesis

One likelihood is that the ubiquitin-conjugating enzymes, UBE2D1 and UBE2D2, mediate direct conjugation of ubiquitin onto VEGFR2 as a client protein or substrate. To test this idea, we introduced recombinant human UBE2D1 or UBE2D2 proteins directly into endothelial cells using a technique called proteofection (Figure 6A). Cytoplasmic delivery of recombinant UBE2D1 or UBE2D2 caused ~50% decrease in VEGFR2 levels after 3 h (Figure 6B). These data support roles for both UBE2D1 and UBE2D2 in down-regulating VEGFR2 levels in endothelial cells. Cell surface protein levels of a transmembrane protein (PECAM1) or a GPI-anchored protein (alkaline phosphatase, AP) are not significantly altered by introduction of either UBE2D1 or UBE2D2 into endothelial cells, indicating VEGFR2 specificity.

VEGF-A-stimulated and VEGFR2-regulated signalling normally induces endothelial tubule formation (tubulogenesis), a physiological response which plays a key role in angiogenesis. However, mitogenic signalling is tightly regulated and excessive VEGF-A stimulation can have an inhibitory effect upon angiogenesis (Pontes-Quero et al., 2019). As UBE2D1 or UBE2D2 levels modulate VEGFR2 levels, leading to increased availability and enhanced VEGF-A-regulated signalling, we next asked whether there are effects on VEGF-A-regulated endothelial tubulogenesis. Either UBE2D1 or UBE2D2 depletion caused a substantial increase in endothelial tubulogenesis in both basal and VEGF-A-stimulated conditions (Figure 7A). Evaluation of endothelial tubule length, tubule size and number of branch points (vs. controls) revealed that all these parameters increased upon UBE2D1 or UBE2D2 depletion. There was 4-5-fold increase in basal endothelial tubulogenesis (without VEGF-A treatment; Figure 7B-7D). Upon VEGF-A-stimulation, there was ~3-fold increase in endothelial tubulogenesis upon UBE2D1 or UBE2D2 depletion vs. controls (Figure 7B-7D). These data support roles for UBE2D1 and UBE2D2 in the VEGF-A-regulated endothelial response that contributes to angiogenesis.

Discussion

VEGFR2 represents a class of membrane proteins with embedded enzymatic activity i.e. receptor tyrosine kinases (RTKs), which link ligand binding to signal transduction pathways which control cell function and physiology. Although it is well-documented that VEGFR2 undergoes ubiquitination, the nature of the enzymes that regulate VEGFR2 ubiquitination is ill-defined. In this study, we found that two closely related ubiquitin-conjugating E2 enzymes, UBE2D1 and UBE2D2, regulate VEGFR2 ubiquitination and VEGF-A-regulated endothelial function. This is supported by five lines of evidence. A reverse genetics screen identified UBE2D1 and UBE2D2 as top ranked candidates for effects on VEGFR2 levels. Furthermore, depletion of two closely related homologues, UBE2D3 or UBE2D4, have no effects on VEGFR2 levels. Next, depletion of either UBE2D1 or UBE2D2 causes a rise in plasma membrane VEGFR2 levels that clearly modulates on VEGF-A-regulated signalling pathways. There was a clear increase in VEGF-A stimulated activation of MAPK, PLCγ1 and Akt signalling pathways. Third, both UBE2D1 and UBE2D2 can form complexes with VEGFR2 and promote down-regulation in endothelial cells. Upon depletion of either UBE2D1 or UBE2D2, VEGFR2 recycling between the plasma membrane and endosomes is increased. This implies that reduced VEGFR2 ubiquitination due to reduced UBE2D1 or UBE2D2 facilitates increased trafficking from endosomes back to the plasma membrane. Finally, depletion of UBE2D1 or UBE2D2 promotes endothelial tubulogenesis, an essential requirement in angiogenesis. Interestingly, a physiological response (angiogenesis) is sensitised and elevated under both basal and excess VEGF-A conditions where UBE2D1 or UBE2D2 is depleted.

Previous work shows that VEGF-A stimulates VEGFR2 activation, ubiquitination and degradation (Basagiannis et al., 2017; Bruns et al., 2010; Ewan et al., 2006). However, endothelial cells also utilise a UBA1-dependent pathway to control basal VEGFR2 levels independent of VEGF-A-stimulated VEGFR2 degradation (Smith et al., 2017). Herein, VEGF-A stimulation caused similar rates of VEGFR2 decrease in control, UBE2D1 and UBE2D2-depleted cells, supporting the existence of a separate pathway controlling VEGF-A-stimulated VEGFR2 ubiquitination. One interpretation is that UBA1 working alongside UBE2D1 or UBE2D2 and a hitherto uncharacterised E3 ubiquitin ligase, facilitates the transfer of ubiquitin to VEGFR2 which subsequently modulates membrane receptor trafficking and proteolysis. Such regulation influences VEGFR2 bioavailability at the plasma membrane. Our postulated mechanism could have wider implications, as epidermal growth factor receptor (EGFR) is also noted to undergo

ubiquitination and degradation (Katz et al., 2002) without tyrosine kinase activation (Opresko et al., 1995).

The enhanced bioavailability of VEGFR2 at the plasma membrane caused by UBE2D1 or UBE2D2 knockdown allows an increase in specific signalling output through PLCγ1, Akt and ERK1/2 phosphorylation. However, it is interesting to note that p38 MAPK activation, a key target of VEGF-A stimulation is not affected by this rise in VEGFR2 levels. In this context, our previous work demonstrates that p38 MAPK activation is independent of canonical MAPK and PI3K-Akt signalling pathways (Fearnley et al., 2016). Knockdown of clathrin heavy chain CHC17 levels which blocks clathrin-dependent endocytosis markedly inhibits VEGF-A-dependent Akt and ERK1/2 activation, but p38 MAPK levels are not affected (Fearnley et al., 2016). Such findings highlight clathrin-dependence for canonical MAPK and PI3K-Akt signalling, whereas p38 MAPK activation occurs via a different route. In the context of this study, elevated VEGFR2 levels is due to a lack of basal ubiquitination by UBE2D1 and/or UBE2D2: upon VEGF-A stimulation, an increase in clathrin-dependent VEGFR2 endocytosis promotes canonical MAPK and PI3K-Akt signalling events.

The intracellular location of UBE2D-regulated VEGFR2 ubiquitination remains to be determined. One likelihood is that plasma membrane VEGFR2 levels are increased upon depleted UBE2D1 or UBE2D2 levels associated with endocytic pathway i.e. plasma membrane and/or endosomes. Alternatively, biosynthetic VEGFR2 could be targeted for ubiquitination and degradation by an E3 ubiquitin ligase, RNF121 (Maghsoudlou et al., 2016). Thus although the exact location of UBE2D1 and UBE2D2–mediated VEGFR2 ubiquitination is unclear, this pathway modulates VEGFR2 trafficking in the endosome-lysosome network which impacts on proteolysis.

One likelihood is that UBE2D1 and UBE2D1 interact with UBA1, one of the major E1 ubiquitin-activating enzymes. Previous studies have shown that UBA1 depletion increases plasma membrane VEGFR2 levels, with similar effects on VEGF-A-stimulated signal transduction and tubulogenesis (Smith et al., 2017). UBA1 interactions with UBE2D1 or UBE2D2 are well-documented (Jin et al., 2007), and involved in the ubiquitination of 100-200 client proteins or substrates (www.thebiogrid.org). Interestingly, we can detect a stable UBE2D-VEGFR2 complex in endothelial cells, which likely includes E1 and E3 enzymes. The identity of the E3 ubiquitin ligase in this complex remains unclear. A number of studies suggest a variety of E3 ubiquitin ligases which regulate VEGFR2 including Cbl, βTrcP and RNF121 (Duval et al., 2003; Maghsoudlou et al., 2016;

Shaik et al., 2012). More work is needed to identify the exact composition and properties of the E1-E2-E3 complex that binds VEGFR2 in endothelial cells.

Both UBE2D1 and UBE2D2 are widely expressed enzymes with a large number of interactions and client substrates linked to different cellular processes. Our work showing roles for UBE2D1 and UBE2D2 in controlling VEGFR2 levels highlights roles for specific E2 ubiquitin-conjugating enzymes in angiogenesis. Whilst E2 knockdown demonstrates a significant VEGFR2 dependent effect on tubulogenesis, there is also the potential for other signalling pathways to influence this process. It is significant that endothelial tubule formation is also elevated without addition of exogenous VEGF-A in UBE2D1 and UBE2D2 knockdown endothelial cells. Endothelial growth medium contains low levels of VEGF-A (3-5ng/ml) and other growth factors/hormones of uncertain concentration that are needed for endothelial cell homeostasis and survival. This is likely to result in increased tubulogenesis via signals through both VEGFR2 and other pathways. In E2 depleted cells, these signals are likely to be enhanced at least in part due to elevated VEGFR2 levels. It is interesting to observe however that there must be additional targets for these E2s that influence angiogenesis. The identity of these factors and the mechanisms by which they exert this effect remain to be investigated. As a case in point, hypoxia-responsive angiogenesis in skeletal muscle is impaired when UBE2D1 levels are elevated upon TNFα stimulation (Basic et al., 2014). Our findings support a role of UBE2D1 and UBE2D2 as regulators of angiogenesis through a direct effect on VEGFR2 levels and bioavailability at the plasma membrane.

Materials and Methods

Cell culture and materials

Primary HUVECs were isolated from the umbilical cords of patients undergoing elective Caesarean section at Leeds General Infirmary (Leeds, UK) and who provided informed consent (Ethical approval reference CA03/020 from Leeds NHS Hospitals Local Ethics Committee). HUVECs were cultured as previously described (Howell et al., 2004). HUVECs, endothelial cell growth medium (ECGM), primary normal dermal human fibroblasts and human recombinant VEGF-A_{165} were obtained from PromoCell (Heidelberg, Germany). MCDB131 medium, OptiMEM, DMEM and AlexaFluor-conjugated secondary antibodies were obtained from Thermo Fisher Scientific (Waltham, USA). Antibodies were sourced as follows: goat polyclonal anti-VEGFR2 (R&D Systems, Minneapolis, USA), mouse HRP-conjugated anti-α-tubulin

(Proteintech, Rosemont, USA), rabbit anti-phospho (Y1175) VEGFR2, rabbit antibodies to total and phosphorylated forms of p38, Akt, PLCγ1 and ERK (Cell Signalling Technologies, Danvers, USA), mouse anti-PECAM1 (BioLegend, San Diego, USA), rabbit anti-UBE2D1 and rabbit anti-UBE2D2 (Abcam, Cambridge, UK), mouse anti-transferrin receptor (Santa Cruz Biotechnology, Dallas, USA) and mouse anti-ubiquitin (2BScientific, Upper Heyford, UK). Purified rabbit anti-alkaline phosphatase antibody was obtained from A. Booth (University of Leeds, UK). HRP-conjugated secondary antibodies were obtained from Stratech Scientific (Newmarket, UK). RIPA buffer with EDTA was obtained from Alfa Aesar (Massachusetts, USA). ON-TargetPlus siRNA duplexes were obtained from Horizon Discovery (Cambridge, UK). Pro-DeliverIN protein delivery reagent was obtained from OZ Biosciences (Marseille, France). Protein G agarose beads were obtained from Merck Millipore (Burlington, USA). Cell lysis buffer was obtained from Cell Signalling Technologies (Danvers, USA). Duolink proximity ligation assay kit was purchased from Sigma-Aldrich (Dorset, UK).

E2 ubiquitin ligase siRNA library

An E2 conjugating enzyme database was collated to include all validated, putative and catalytically inactive forms. For the screen, E2 library plates were produced by adding 50 nM SMARTpool siRNA (4 duplexes per target) specific for each E2 to separate wells. A separate 96-well library plate was used for each experiment.

Screening of E2 knockdown on VEGFR2 levels

HUVECs were reverse transfected in 96-well plates grown in serum-free OptiMEM medium with 0.1 µl per well Lipofectamine RNAiMAX and a 50 nM SMARTpool siRNA, specific for an E2 enzyme or non-targeting control. Mock-transfected (treated with Lipofectamine RNAiMAX only) and untreated HUVECs were included as controls. HUVECs were incubated with lipid-siRNA complexes for 6 h at 37°C before replacement of OptiMEM with fresh ECGM. After 72 h, cells were processed for immunofluorescence microscopy.

Immunofluorescence microscopy

HUVECs were fixed in 3% (w/v) paraformaldehyde followed by brief permeabilisation in 0.1% (w/v) Triton X-100. Cells were incubated overnight at room temperature with primary antibodies in 1 mg/ml BSA in PBS before addition of DAPI and AlexaFluor488- or AlexaFluor594-conjugated secondary antibodies for 2 h. Images were acquired using an

EVOS FL Auto 2 inverted digital microscope (Thermo Fisher Scientific), with 3 fields of view obtained per condition. Fluorescence intensity was calculated using ImageJ version 1.46r (National Institutes of Health, USA).

Co-immunoprecipitation

HUVECs were treated as required prior to washing with ice cold PBS, flash crosslinking with 0.4% paraformaldehyde for 1 minutes and lysis with RIPA buffer plus EDTA, supplemented with 1mM PMSF and protease inhibitor cocktail. Equal amounts of lysate were incubated overnight at 4°C with 1ug appropriate rabbit primary antibodies or without antibodies (control). Protein G agarose was added and incubated at 4°C for 2 hours. Beads were washed 3 times with 0.1X RIPA buffer plus EDTA, pelleted and resuspended in 20µl LDS sample buffer for immunoblotting.

Immunoblotting

HUVECs were treated as required before washing with ice cold PBS and lysis in 2% (w/v) SDS in PBS supplemented with protease inhibitor cocktail and 1 mM PMSF. The bicinchoninic acid assay was utilised to quantify protein before 25µg per lane was loaded onto 10% or 6-20% gradient SDS-PAGE gel. The gel was run at 110 V for approximately 2 h until sufficiently separated. Proteins were transferred overnight at 4°C onto nitrocellulose membrane at 50 mA current. Membranes were blocked in 5 mg/ml BSA in TBS-T then incubated with primary antibody in 1 mg/ml BSA in TBS-T overnight at 4°C before incubation with donkey HRP-conjugated secondary antibodies for 1 h at room temperature. Immunoblots were developed by enhanced chemiluminescence and detected on a G:Box imaging system (Syngene, Cambridge, UK). ImageJ was used to quantify pixel intensity and normalised against tubulin as loading control.

Proteofection of primary endothelial cells

Delivery of human recombinant protein was achieved by transfection of 50% confluent HUVECs in 24-well plates. Recombinant protein (1 µg/well) was diluted in PBS to 100µg/ml before combining with Pro-DeliverIN transfection reagent (2 µl/well) and incubating for 15 min at room temperature. OptiMEM was then added at 100 µl/well before immediately adding dropwise onto growing HUVECs. After 3 h incubation at 37°C, the cells were twice washed with ice cold PBS before lysis in 2% (w/v) SDS for immunoblotting.

Endothelial tubulogenesis assay

Fibroblasts were grown to confluency in DMEM supplemented with 10% (v/v) fetal bovine serum, 1 mM sodium pyruvate and 1 mM non-essential amino acids. HUVECs were reverse transfected in a 96-well plate as described above. 24 h after transfection, the HUVECs were trypsinised and 5000 cells per well added onto the fibroblast monolayer in duplicate. The cells were incubated for 7 days at 37°C in a 1:1 ratio of ECGM and DMEM with or without 25 ng/ml VEGF-A_{165} supplementation (added every 2 days). After 7 days growth, the cells were washed with PBS before fixation in 3% (w/v) paraformaldehyde without permeabilisation for immunofluorescence analysis. PECAM-1 staining was used to allow visualisation of endothelial tubules. Endothelial tubule length, size (representative of tubule area as a function of length and thickness) and number of branch points were quantified using AngioQuant software version 1.33(Niemisto et al., 2005).

Plasma membrane VEGFR2 recycling

E2 depleted and control HUVECs were serum starved for 2 h in MCDB131 + 0.2% BSA before incubation in goat anti-VEGFR2 primary antibody for 30 min at 37°C. VEGF-A was then added for an additional 30 min. Cell surface primary antibody was stripped by acid wash with serum-free MCDB131 at pH 2 at 4°C followed by two washes in normal MCDB131. Cells were incubated with donkey anti-sheep AlexaFluor488-conjugated secondary antibody for 30 min at 37°C before fixation and DAPI addition. Images were acquired using an EVOS-FL inverted digital microscope. Fluorescence intensity was calculated using ImageJ version 1.46r (National Institutes of Health, USA).

Cell surface biotinylation

E2 depleted and control HUVECs were serum starved for 2 h in MCDB131 + 0.2% (w/v) BSA prior to stimulation with 25 ng/ml VEGF-A_{165} at intervals up to 1 h. HUVECs were then washed twice in ice cold PBS before cell surface proteins were biotinylated by 45 min incubation at 4°C with 0.25 mg/ml NHS-biotin in PBS containing 2 mM $CaCl_2$ and 2 mM $MgCl_2$. The biotinylation reaction was quenched with a TBS wash before lysis in buffer containing 1% (v/v) NP-40, 50 mM Tris-HCl pH 7.5, 150 mM NaCl and 1 mM PMSF. NeutraAvidin-agarose beads (ThermoFisher Scientific) were utilised to isolate biotinylated cell surface proteins overnight at 4°C. The agarose beads were washed 3 times with NP-40 buffer before proteins were eluted in SDS sample buffer ready for SDS-PAGE separation and immunoblot analysis.

Acknowledgements

This work was supported by British Heart Foundation project grant PG/16/86/32474 (S.P, M.A.H, I.Z.) and British Heart Foundation PhD studentship FS/12/20/29462 (G.S.).

References

Basagiannis, D., Zografou, S., Galanopoulou, K. and Christoforidis, S. (2017). Dynasore impairs VEGFR2 signalling in an endocytosis-independent manner. *Sci Rep* **7**, 45035.

Basic, V. T., Jacobsen, A., Sirsjo, A. and Abdel-Halim, S. M. (2014). TNF stimulation induces VHL overexpression and impairs angiogenic potential in skeletal muscle myocytes. *Int J Mol Med* **34**, 228-36.

Bruns, A. F., Herbert, S. P., Odell, A. F., Jopling, H. M., Hooper, N. M., Zachary, I. C., Walker, J. H. and Ponnambalam, S. (2010). Ligand-stimulated VEGFR2 signaling is regulated by co-ordinated trafficking and proteolysis. *Traffic* **11**, 161-74.

Chung, A. S. and Ferrara, N. (2011). Developmental and pathological angiogenesis. *Annu Rev Cell Dev Biol* **27**, 563-84.

Critchley, W. R., Pellet-Many, C., Ringham-Terry, B., Harrison, M. A., Zachary, I. C. and Ponnambalam, S. (2018). Receptor Tyrosine Kinase Ubiquitination and De-Ubiquitination in Signal Transduction and Receptor Trafficking. *Cells* **7**.

De Palma, M., Biziato, D. and Petrova, T. V. (2017). Microenvironmental regulation of tumour angiogenesis. *Nat Rev Cancer* **17**, 457-474.

Duval, M., Bedard-Goulet, S., Delisle, C. and Gratton, J. P. (2003). Vascular endothelial growth factor-dependent down-regulation of Flk-1/KDR involves Cbl-mediated ubiquitination. Consequences on nitric oxide production from endothelial cells. *J Biol Chem* **278**, 20091-7.

Ewan, L. C., Jopling, H. M., Jia, H., Mittar, S., Bagherzadeh, A., Howell, G. J., Walker, J. H., Zachary, I. C. and Ponnambalam, S. (2006). Intrinsic tyrosine kinase activity is required for vascular endothelial growth factor receptor 2 ubiquitination, sorting and degradation in endothelial cells. *Traffic* **7**, 1270-82.

Fearnley, G. W., Smith, G. A., Abdul-Zani, I., Yuldasheva, N., Mughal, N. A., Homer-Vanniasinkam, S., Kearney, M. T., Zachary, I. C., Tomlinson, D. C., Harrison, M. A. et al. (2016). VEGF-A isoforms program differential VEGFR2 signal transduction, trafficking and proteolysis. *Biol Open* **5**, 571-83.

Gampel, A., Moss, L., Jones, M. C., Brunton, V., Norman, J. C. and Mellor, H. (2006). VEGF regulates the mobilization of VEGFR2/KDR from an intracellular endothelial storage compartment. *Blood* **108**, 2624-31.

Howell, G. J., Herbert, S. P., Smith, J. M., Mittar, S., Ewan, L. C., Mohammed, M., Hunter, A. R., Simpson, N., Turner, A. J., Zachary, I. et al. (2004). Endothelial cell confluence regulates Weibel-Palade body formation. *Mol Membr Biol* **21**, 413-21.

Jin, J., Li, X., Gygi, S. P. and Harper, J. W. (2007). Dual E1 activation systems for ubiquitin differentially regulate E2 enzyme charging. *Nature* **447**, 1135-8.

Jopling, H. M., Howell, G. J., Gamper, N. and Ponnambalam, S. (2011). The VEGFR2 receptor tyrosine kinase undergoes constitutive endosome-to-plasma membrane recycling. *Biochemical and biophysical research communications* **410**, 170-176.

Jopling, H. M., Odell, A. F., Pellet-Many, C., Latham, A. M., Frankel, P., Sivaprasadarao, A., Walker, J. H., Zachary, I. C. and Ponnambalam, S. (2014). Endosome-to-Plasma Membrane Recycling of VEGFR2 Receptor Tyrosine Kinase Regulates Endothelial Function and Blood Vessel Formation. *Cells* **3**, 363-85.

Katz, M., Shtiegman, K., Tal-Or, P., Yakir, L., Mosesson, Y., Harari, D., Machluf, Y., Asao, H., Jovin, T., Sugamura, K. et al. (2002). Ligand-independent degradation of epidermal growth factor receptor involves receptor ubiquitylation and Hgs, an adaptor whose ubiquitin-interacting motif targets ubiquitylation by Nedd4. *Traffic* **3**, 740-51.

Khurana, R., Simons, M., Martin, J. F. and Zachary, I. C. (2005). Role of angiogenesis in cardiovascular disease: a critical appraisal. *Circulation* **112**, 1813-24.

Lampugnani, M. G., Orsenigo, F., Gagliani, M. C., Tacchetti, C. and Dejana, E. (2006). Vascular endothelial cadherin controls VEGFR-2 internalization and signaling from intracellular compartments. *J Cell Biol* **174**, 593-604.

Maghsoudlou, A., Meyer, R. D., Rezazadeh, K., Arafa, E., Pudney, J., Hartsough, E. and Rahimi, N. (2016). RNF121 Inhibits Angiogenic Growth Factor Signaling by Restricting Cell Surface Expression of VEGFR-2. *Traffic* **17**, 289-300.

Martin, A., Komada, M. R. and Sane, D. C. (2003). Abnormal angiogenesis in diabetes mellitus. *Med Res Rev* **23**, 117-45.

Murdaca, J., Treins, C., Monthouel-Kartmann, M. N., Pontier-Bres, R., Kumar, S., Van Obberghen, E. and Giorgetti-Peraldi, S. (2004). Grb10 prevents Nedd4-mediated vascular endothelial growth factor receptor-2 degradation. *J Biol Chem* **279**, 26754-61.

Niemisto, A., Dunmire, V., Yli-Harja, O., Zhang, W. and Shmulevich, I. (2005). Robust quantification of in vitro angiogenesis through image analysis. *IEEE Trans Med Imaging* **24**, 549-53.

Opresko, L. K., Chang, C. P., Will, B. H., Burke, P. M., Gill, G. N. and Wiley, H. S. (1995). Endocytosis and lysosomal targeting of epidermal growth factor receptors are mediated by distinct sequences independent of the tyrosine kinase domain. *J Biol Chem* **270**, 4325-33.

Pontes-Quero, S., Fernández-Chacón, M., Luo, W., Lunella, F. F., Casquero-Garcia, V., Garcia-Gonzalez, I., Hermoso, A., Rocha, S. F., Bansal, M. and Benedito, R. (2019). High mitogenic stimulation arrests angiogenesis. *Nat Commun* **10**, 2016.

Sakaue, T., Sakakibara, I., Uesugi, T., Fujisaki, A., Nakashiro, K. I., Hamakawa, H., Kubota, E., Joh, T., Imai, Y., Izutani, H. et al. (2017). The CUL3-SPOP-DAXX axis is a novel regulator of VEGFR2 expression in vascular endothelial cells. *Sci Rep* **7**, 42845.

Scheffner, M., Nuber, U. and Huibregtse, J. M. (1995). Protein ubiquitination involving an E1-E2-E3 enzyme ubiquitin thioester cascade. *Nature* **373**, 81-3.

Shaik, S., Nucera, C., Inuzuka, H., Gao, D., Garnaas, M., Frechette, G., Harris, L., Wan, L., Fukushima, H., Husain, A. et al. (2012). SCF(beta-TRCP) suppresses angiogenesis and thyroid cancer cell migration by promoting ubiquitination and destruction of VEGF receptor 2. *J Exp Med* **209**, 1289-307.

Smith, G. A., Fearnley, G. W., Abdul-Zani, I., Wheatcroft, S. B., Tomlinson, D. C., Harrison, M. A. and Ponnambalam, S. (2017). Ubiquitination of basal VEGFR2 regulates signal transduction and endothelial function. *Biol Open* **6**, 1404-1415.

Figures

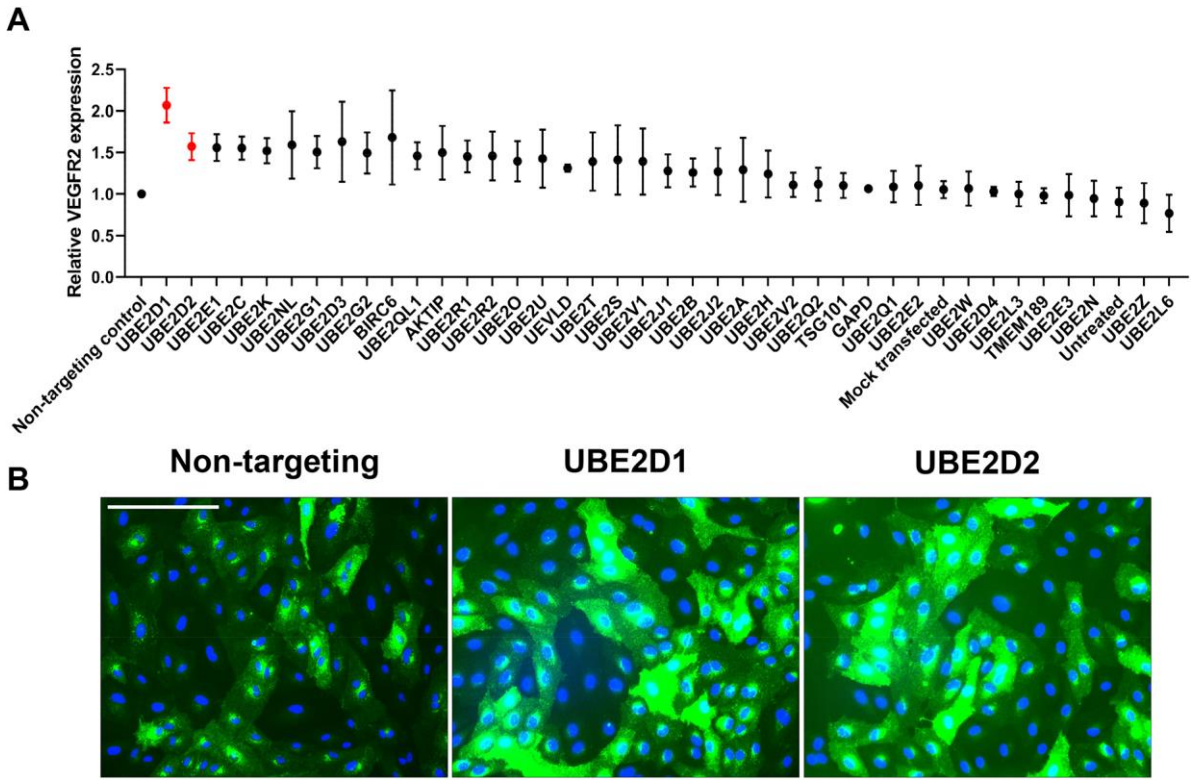

Fig. 1. Reverse genetics screen of E2 ubiquitin-conjugating enzyme family on total VEGFR2 levels in endothelial cells. (A) E2 ubiquitin-conjugating enzyme screen in primary endothelial cells. Histogram quantification of effects of E2 knockdown on total VEGFR2 levels in endothelial cells (see Materials and Methods). (B) Analysis of basal total VEGFR2 levels in endothelial cells after no transfection, transfection with control non-targeting, UBE2D1 or UBE2D2-specific siRNA duplexes followed by immunofluorescence microscopy to detect total VEGFR2 (green) or nuclear DNA (blue). Representative images from repeat experiments (n=3). Bar, 200 μm.

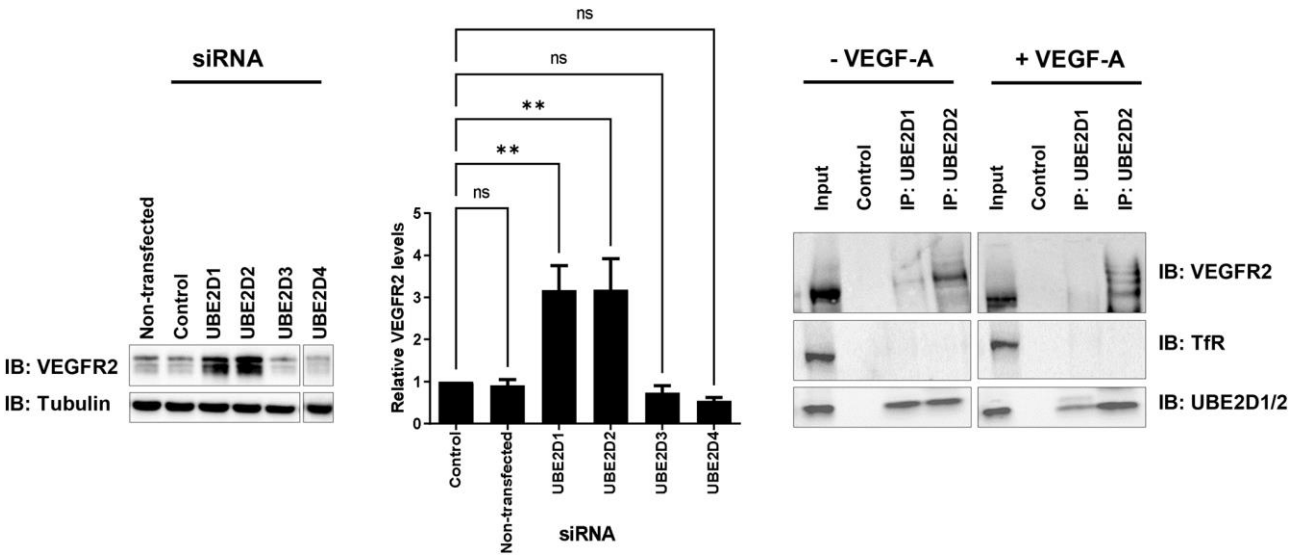

Fig. 2. UBE2D1 and UBE2D2 knockdown stimulates VEGFR2 protein levels in endothelial cells. (A) Immunoblot analysis of basal total VEGFR2 levels in endothelial cells after treatment with control non-targeting, UBE2D1, UBE2D2, UBE2D3 or UBE2D4-specific siRNA duplexes. Antibodies to VEGFR2 and tubulin (control) were used to analyse protein levels. (B) Quantification of immunoblot data of relative VEGFR2 levels in endothelial cells after treatment with control non-targeting, UBE2D1, UBE2D2 or UBE2D3-specific siRNA duplexes (see Materials and Methods). Error bars indicate +SEM. Statistical significance assessed by One-way ANOVA followed by Tukey's post-test for multiple comparisons. Significance indicated by asterisks (*, $p<0.05$; n=3). (C) Immunoblot analysis of co-immunoprecipitation of VEGFR2 with UBE2D1 and UBE2D2 from HUVEC lysate. Transferrin receptor was analysed as a control to ensure specificity of interaction.

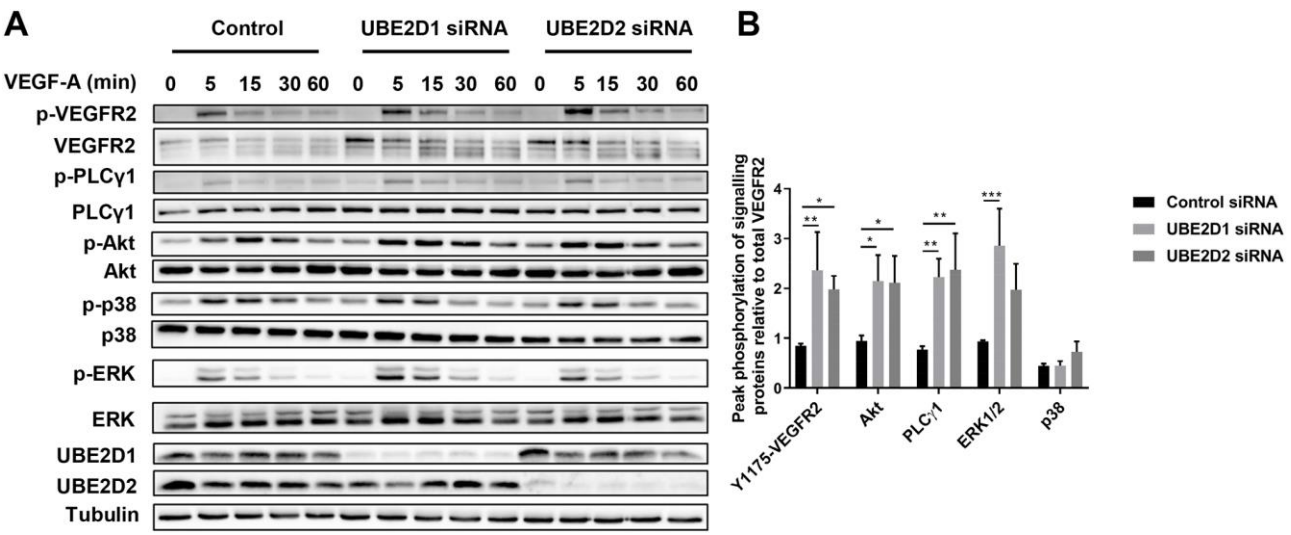

Fig. 3. Elevated VEGFR2 levels caused by UBE2D1 or UBE2D2 knockdown promotes downstream activation and signalling in multiple pathways. (A) Immunoblot analysis of VEGF-A stimulated signalling events after transfection with control non-targeting, UBE2D1 or UBE2D2 siRNA. (B) Quantification of immunoblot data for VEGF-A-regulated signal transduction by monitoring maximal levels of phosphorylated VEGFR2, Akt, PLCγ1, p38 and ERK in primary endothelial cells transfected with control non-targeting, UBE2D1 or UBE2D2 siRNA. Error bars indicate +SEM (n=3). Significance was determined by two-way ANOVA followed by Dunnett's post-test for multiple comparisons and indicated by asterisks (*, p<0.05; **, p<0.01; ***, p<0.001; ****, p<0.0001).

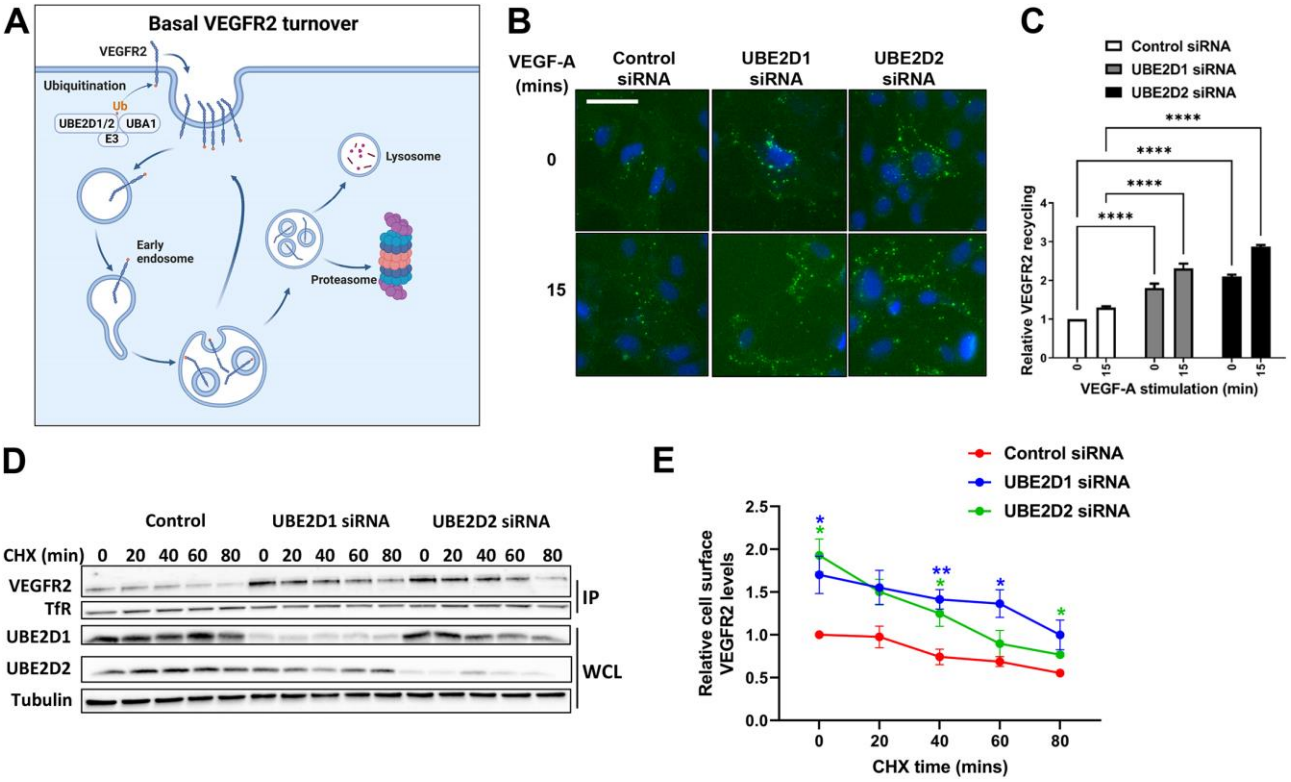

Fig. 4. VEGFR2 recycling between plasma membrane and endosomes dependence on UBE2D1 and UBE2D2. (A) Schematic overview of VEGFR2 internalization and degradation mediated by basal ubiquitination without stimulation. (B) Immunofluorescence analysis of VEGFR2 recycling to the plasma membrane after depletion of UBE2D1 or UBE2D2 with and without VEGF-A stimulation. Bar, 50 µm. (C) Quantification of relative VEGFR2 recycling from immunofluorescence images in endothelial cells after knockdown with control non-targeting, UBE2D1 or UBE2D2-specific siRNA. Significance was determined by two-way ANOVA followed by Dunnett's post-test for multiple comparisons and indicated by asterisks (****, p<0.0001; n=3). (D) Analysis of change in plasma membrane VEGFR2 levels determined by cell surface biotinylation assay after cycloheximide treatment in endothelial cells by immunoblotting after transfection with control non-targeting, UBE2D1 or UBE2D2 siRNA. (E) Quantification of relative cell surface VEGFR2 levels in E2-depleted endothelial cells treated with cycloheximide. Significance was determined by two-way ANOVA followed by Dunnett's post-test for multiple comparisons and indicated by asterisks (*, p<0.05; **, p<0.01; n=4).

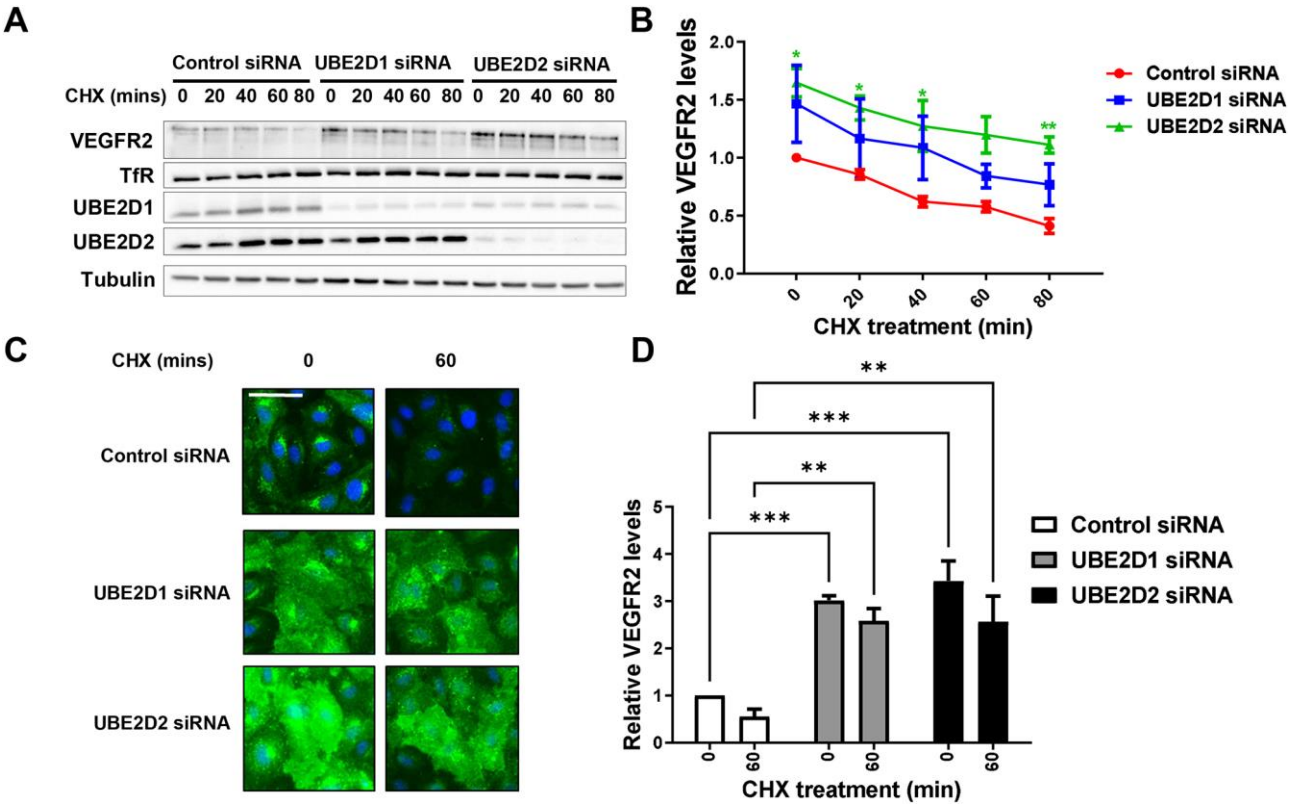

Fig. 5. VEGFR2 levels remain elevated after E2 knockdown despite inhibition of new protein synthesis. (A) Immunoblot analysis of phosphorylated and total VEGFR2 levels after E2 knockdown and treatment with cycloheximide to prevent new protein synthesis, with transferrin receptor levels immunoblotted as control (B) Quantification of immunoblot data of relative VEGFR2 levels after UBE2D1 and UBE2D2 knockdown and cycloheximide treatment. Significance was determined by two-way ANOVA followed by Dunnett's post-test for multiple comparisons and indicated by asterisks (*, p<0.05; **, p<0.01; n=3). (C) Analysis of basal VEGFR2 in primary endothelial cells after E2 knockdown and cycloheximide inhibition of new protein synthesis as measured by immunofluorescence microscopy to detect VEGFR2 (green) or nuclear DNA (blue). Bar, 50 µm. (D) Quantification of immunofluorescence data of relative VEGFR2 levels in primary endothelial cells after control non-targeting, UBE2D1 or UBE2D2 knockdown and cycloheximide treatment (see Materials and Methods). Error bars indicate +SEM. Significance was determined by two-way ANOVA followed by Dunnett's post-test for multiple comparisons and indicated by asterisks (**, p<0.01; ***, p<0.001; n=3).

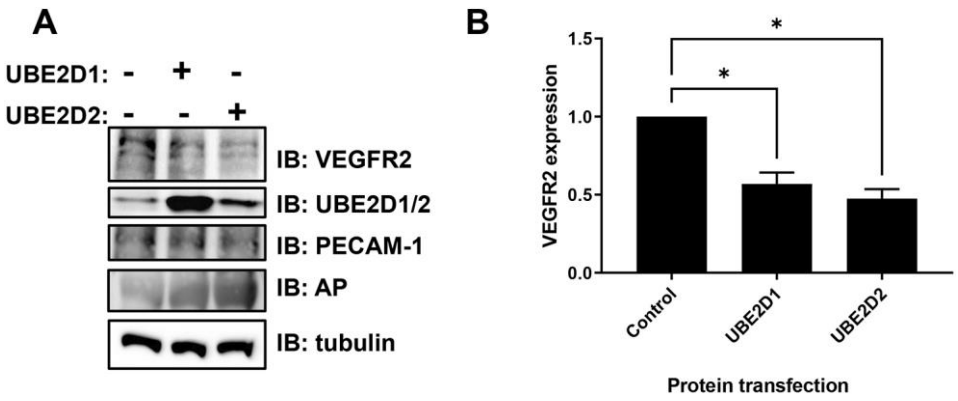

Fig. 6. UBE2D1 and UBE2D2 bind to VEGFR2 and promote down-regulation in endothelial cells. (A) Immunoblot analysis of basal VEGFR2 levels in primary endothelial cells (after 3 h) following proteofection of human recombinant UBE2D1 or UBE2D2 protein compared to control mock proteofection. Antibodies to VEGFR2, UBE2D1, UBE2D2, PECAM-1 and tubulin (control) were used to analyze protein levels. (B) Quantification of immunoblot data of relative VEGFR2 levels in endothelial cells after proteofection with control, UBE2D1 or UBE2D2 recombinant protein. Error bars indicate +SEM. Significance was determined by one-way ANOVA followed by Tukey's post-test for multiple comparisons and indicated by asterisks (*, $p<0.05$; n=4).

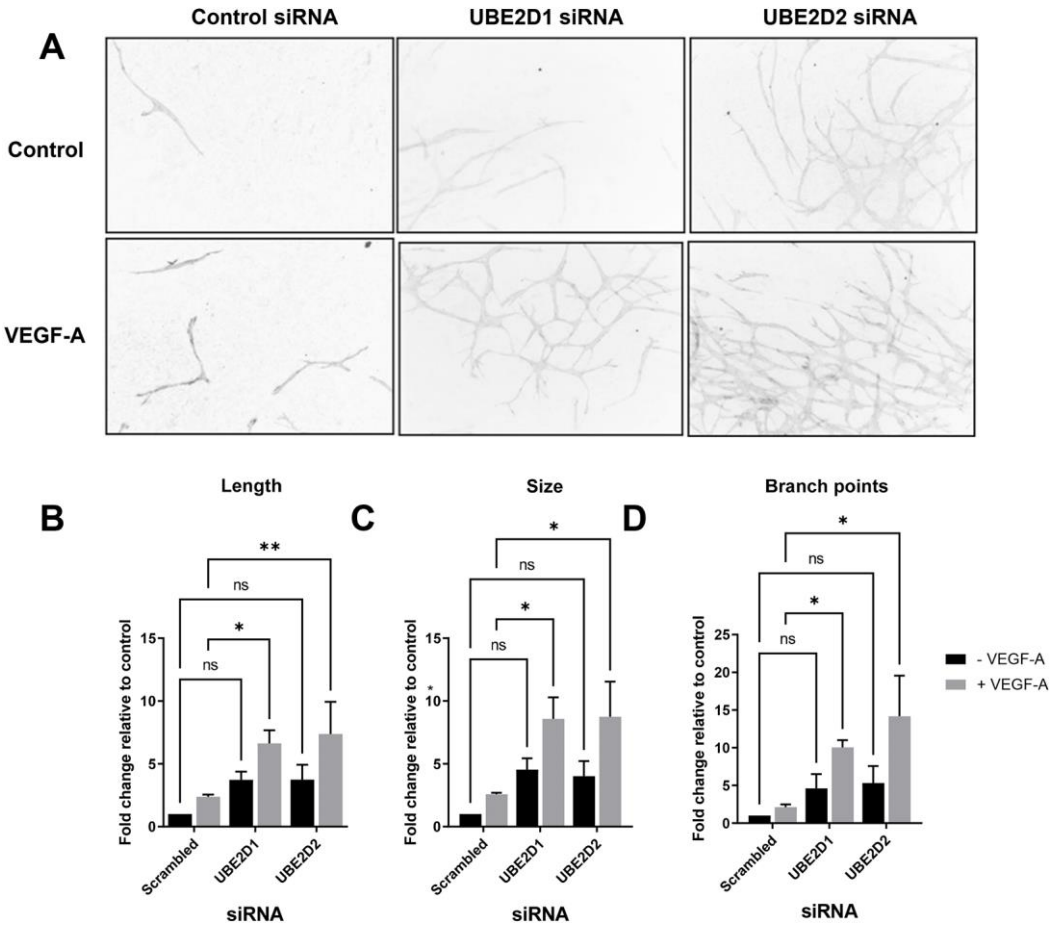

Fig. 7. UBE2D1 and UBE2D2 regulate VEGF-A-stimulated endothelial tubulogenesis. (A) Analysis of tubule formation using a fibroblast-endothelial co-culture assay after transfection of primary endothelial cells with control non-targeting, UBE2D1 or UBE2D2 siRNA in the presence or absence of VEGF-A. (B-D) Quantification of tubulogenesis data for (B) total length, (C) total size, and (D) total number of branch points. Error bars indicate +SEM. Significance was determined by two-way ANOVA followed by Dunnett's post-test for multiple comparisons and indicated by asterisks (*, p<0.05; **, p<0.01; n=3).

Fig. 2A

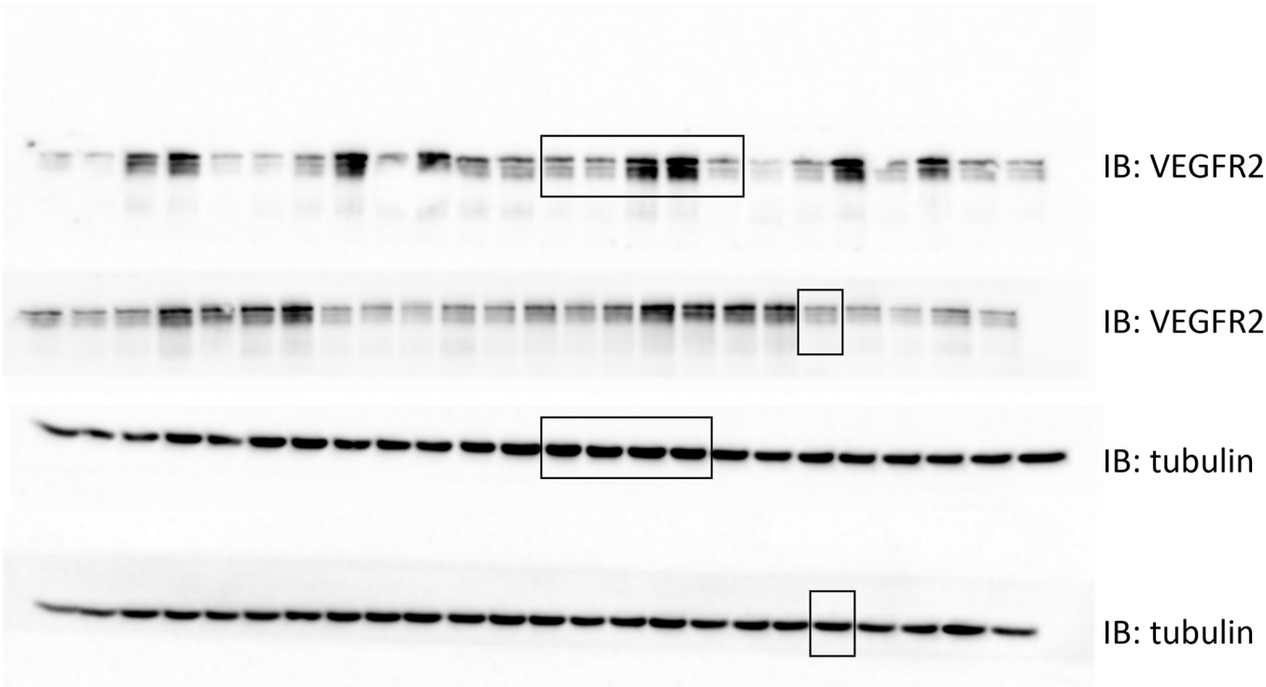

Fig. 2B

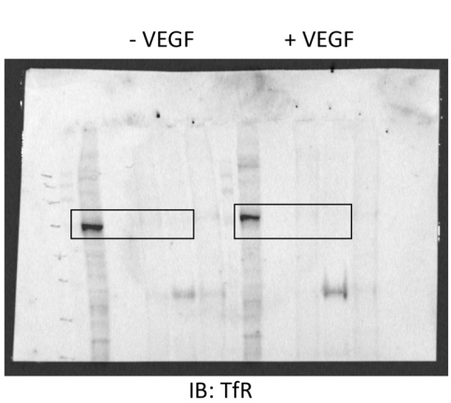

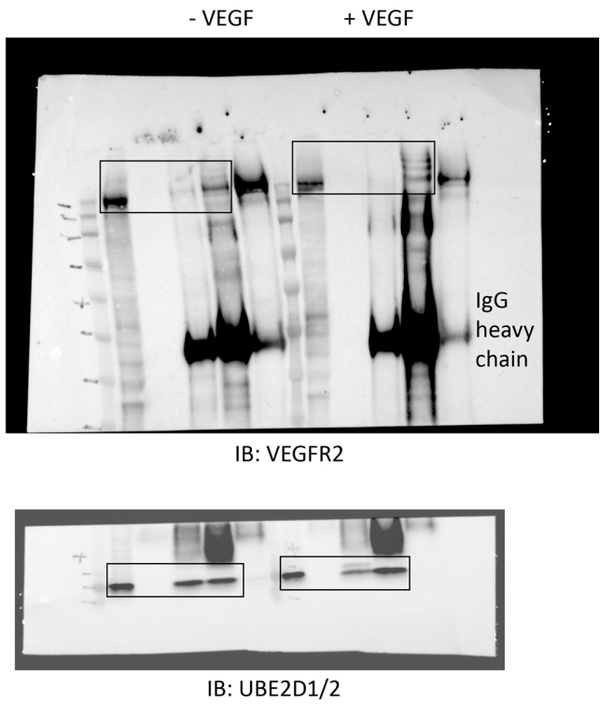

Fig. 3A

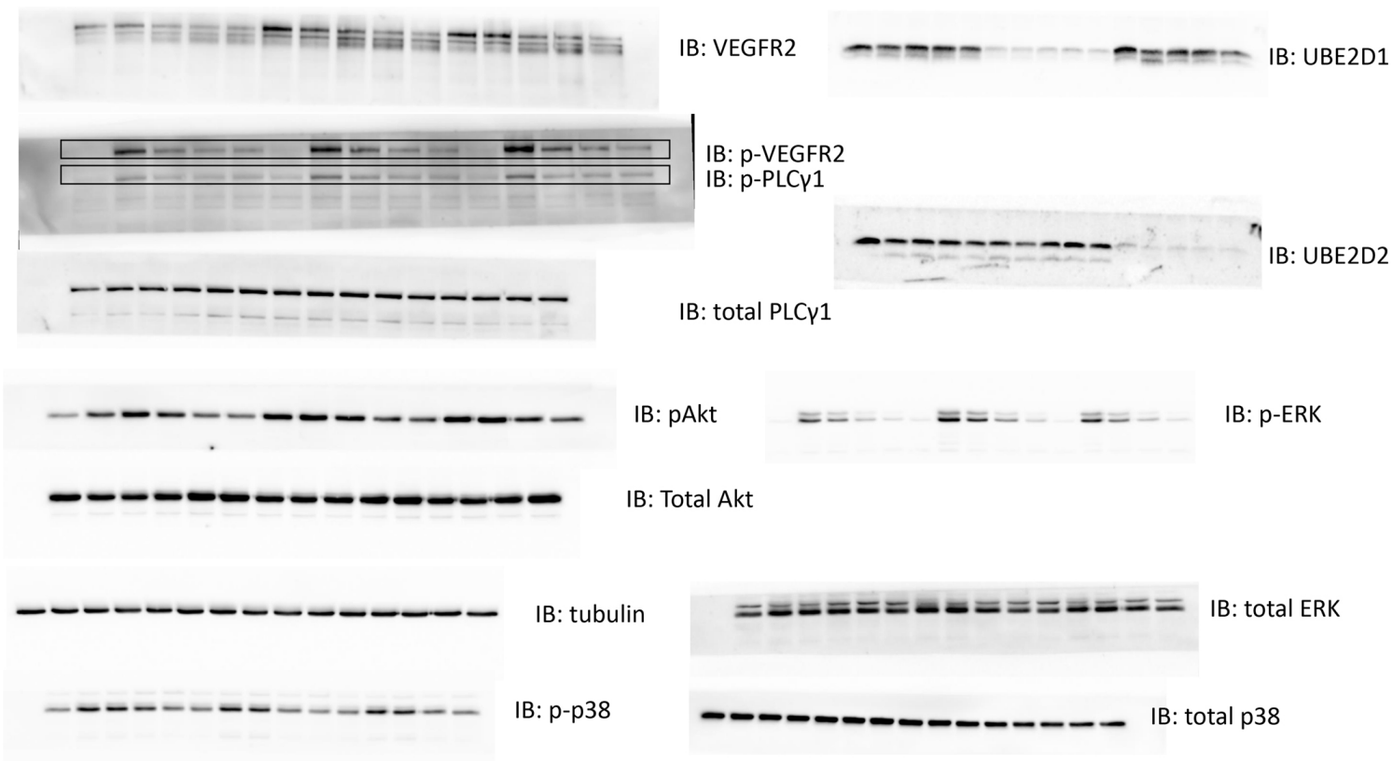

Fig. 4D

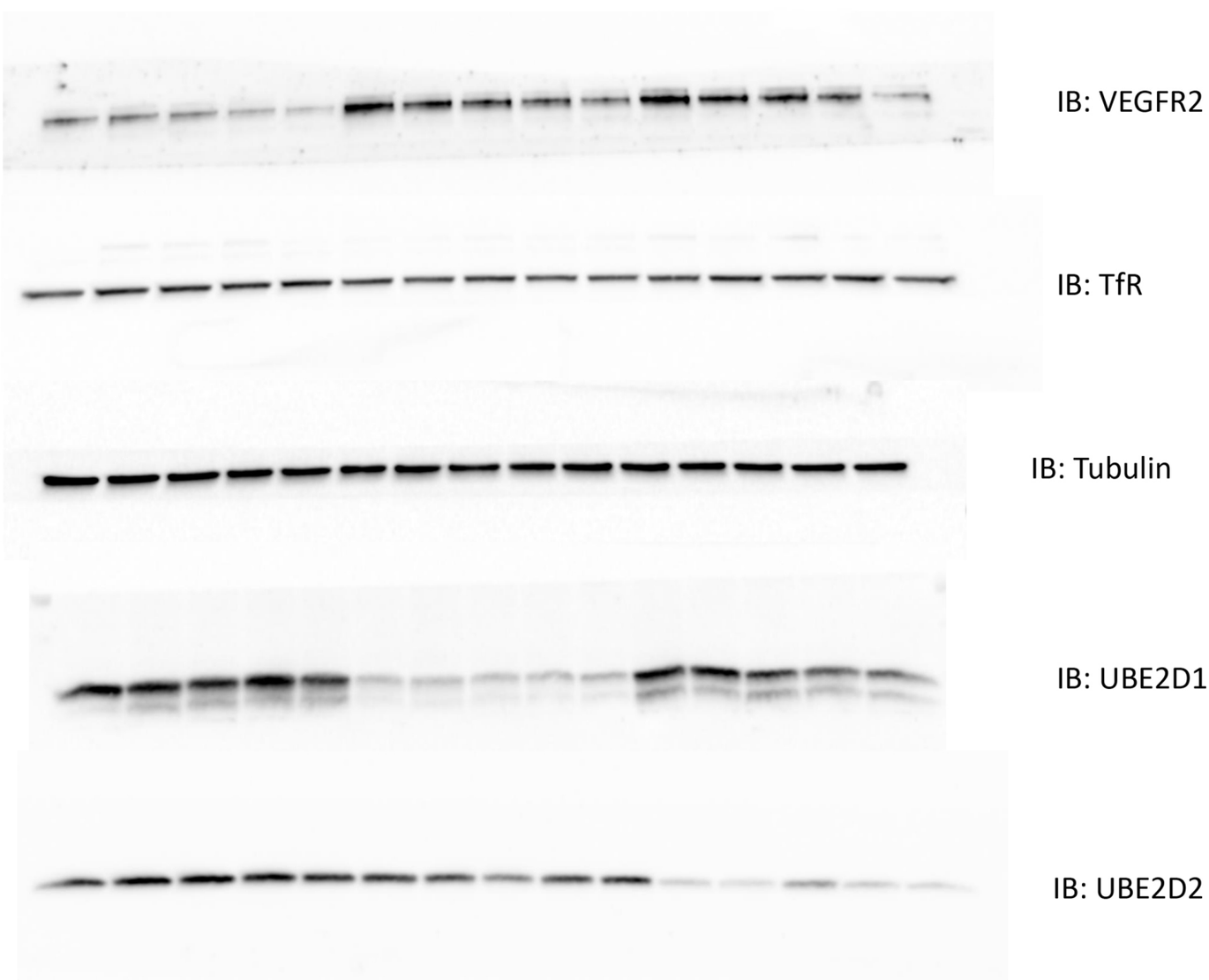

Fig. 5A

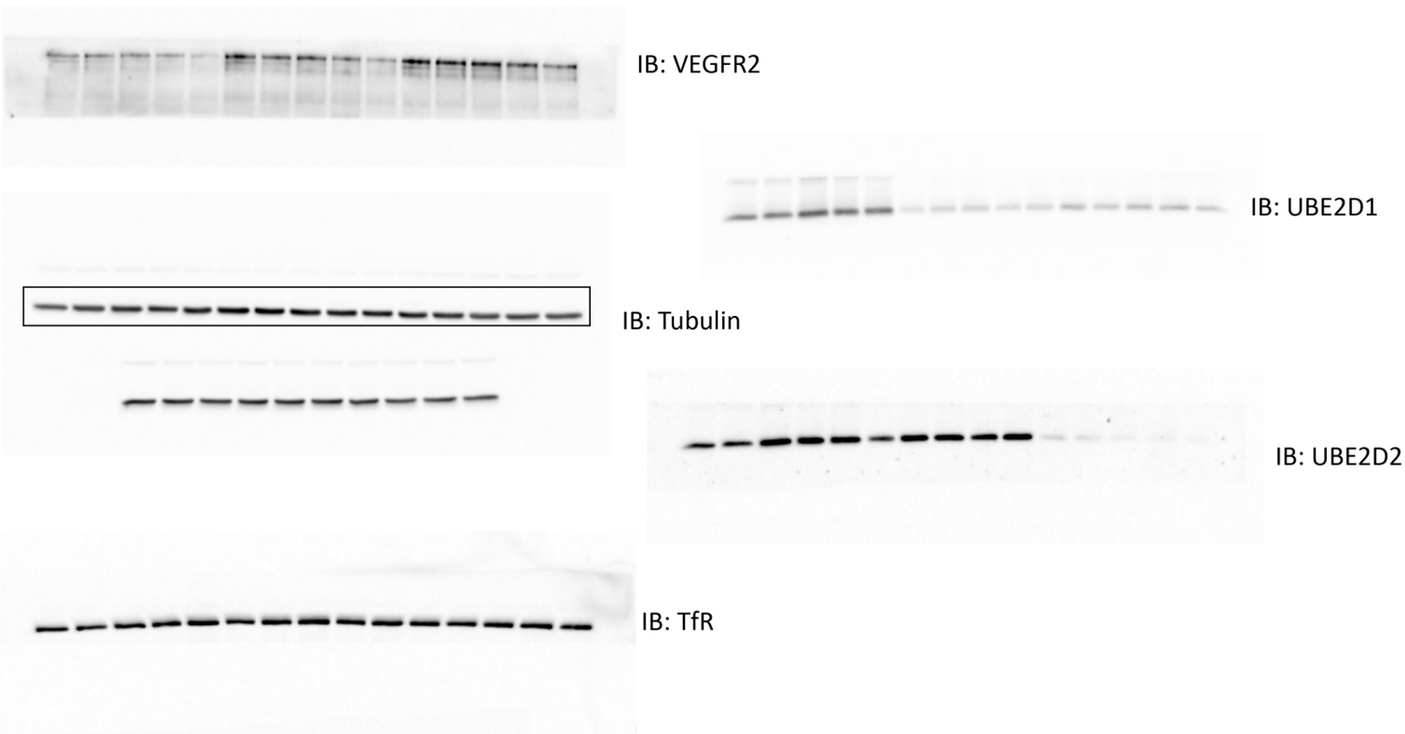

Fig. 6A

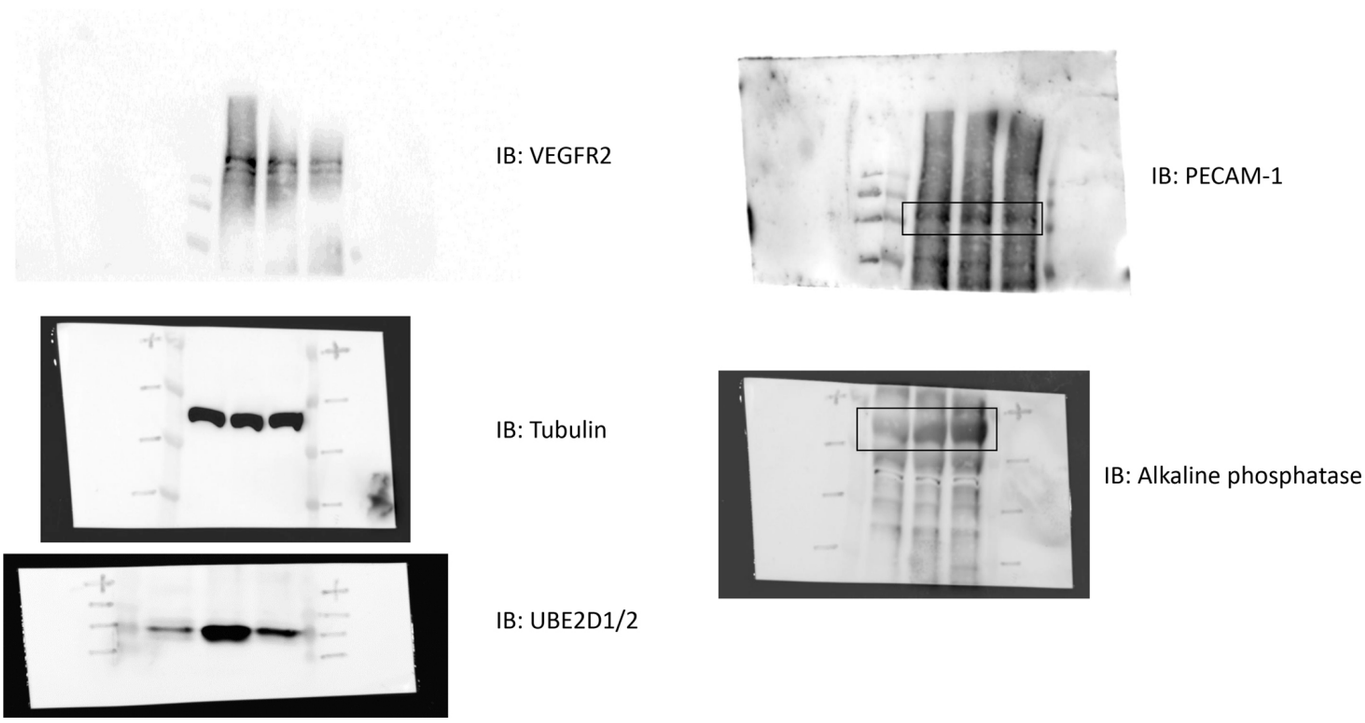

Fig. S1. Blot transparency.